

Improving Fairness in Deepfake Detection*

Yan Ju^{1†}, Shu Hu^{2†‡}, Shan Jia¹, George H. Chen³, Siwei Lyu^{1‡}

¹ University at Buffalo, State University of New York {yanju, shanjia, siweilyu}@buffalo.edu

² Indiana University–Purdue University Indianapolis hu968@purdue.edu

³ Carnegie Mellon University georgechen@cmu.edu

Abstract

Despite the development of effective deepfake detection models in recent years, several recent studies have demonstrated that biases in the training data utilized to develop deepfake detection models can lead to unfair performance for demographic groups of different races and/or genders. Such can result in these groups being unfairly targeted or excluded from detection, allowing misclassified deepfakes to manipulate public opinion and erode trust in the model. While these studies have focused on identifying and evaluating the unfairness in deepfake detection, no methods have been developed to address the fairness issue of deepfake detection at the algorithm level. In this work, we make the first attempt to improve deepfake detection fairness by proposing novel loss functions to train fair deepfake detection models in ways that are agnostic or aware of demographic factors. Extensive experiments on four deepfake datasets and five deepfake detectors demonstrate the effectiveness and flexibility of our approach in improving deepfake detection fairness. The code is available at https://github.com/littlejuyan/DF_Fairness.

1. Introduction

The term deepfakes are often used to refer to realistic images and videos of human faces that are manipulated or generated using deep learning technologies. Several types of deep neural network models such as Variational Autoencoder (VAE) [29, 54], Generative Adversarial Networks (GANs) [16, 24], and diffusion models [8, 49, 55], are used to create deepfakes. Concerns have been raised about deepfakes being used for malicious purposes, such as in political propaganda or cyberattacks. For example, a deepfake video has the ability to depict a world leader engaging in words or actions that never occurred in reality [2], potentially resulting in severe outcomes like the dissemination of misinformation or deceiving the public. To mitigate the impact of

deepfakes, a variety of detection models have been designed with promising detection performance [6, 32, 36, 42, 57, 66]. Currently, the top-performing deepfake detection methods are all based on data-driven and deep learning-based approaches.

Nevertheless, several recent works and reports [36, 40, 53, 60, 62] have shown some fairness issues in current deepfake detection methods, in particular, the performance is not consistent for different demographic groups of gender, age, and ethnicity [62]. For example, several state-of-the-art detectors have higher accuracy for deepfakes with lighter skin tones than those with darker skin tones [21, 53]. A potential reason for unfair detection could be the unbalanced distribution of demographic groups in the training data [40]. However, augmenting the dataset is not a feasible solution due to the significant increase in cost and labor [27]. The conventional bias reduction methods (e.g., [38]) in general computer vision tasks can be applied but deepfake detection poses unique challenges. In particular, we have to cope with the imbalanced distributions of real and deepfake samples, as well as imbalanced distributions across demographic groups.

In this work, we describe two Fair Deepfake Detection (FDD) methods to fill this void. The first one does not rely on demographic details and employs distributionally robust optimization (DRO) [45]. The second one leverages demographic information and employs the fairness risk measure [61]. We term them DAG-FDD (Demographic-agnostic FDD) and DAW-FDD (Demographic-aware FDD), respectively. Specifically, we investigate a DRO technique called *Conditional Value-at-Risk* (CVaR) [31, 48] and demonstrate that it provides a rigorous and tight upper bound on the worst-case risk among subgroups. Our DAG-FDD approach enables deepfake detection modelers to specify a probability threshold for a minority subgroup without explicitly identifying all possible subgroups. The goal is to ensure that all subgroups with at least a specified occurrence probability have low error. Moreover, we explore CVaR as a fairness risk measure by considering the demographic information of different subgroups at the sub-

*This paper has been accepted by WACV 2024

†Equal contribution

‡Corresponding authors

group level, which can balance fairness and accuracy. We also analyze the robustness of CVaR at the sample level in the presence of an imbalanced sample problem, such as the case of fake vs real data in each subgroup. By jointly considering fairness, accuracy, and robustness, our DAW-FDD approach provides a more comprehensive and effective way of achieving fair deepfake detection. Since our learning objectives are based on CVaR, which is a convex function, they can encourage the discovery of many equally effective local optima, even if the model is nonlinear.

The technical novelty of our methods is threefold. **1) Formulation:** CVaR is not commonly used in fairness. When it is used, it usually emphasizes inter-subgroup fairness while overlooking intra-subgroup fairness. We introduced DAW-FDD, a bi-level fairness approach, to address subgroup unfairness and real-fake sample imbalances simultaneously. In particular, our method uses average top- k loss to improve intra-subgroup fairness and model robustness. **2) Optimization:** Optimizing this bi-level loss is non-trivial due to time-consuming ranking operations and varying k values across subgroups. We theoretically proved in Theorem 1 that average top- k is equivalent to the empirical CVaR, eliminating the need for ranking and enabling efficient optimization with uniform α_i values on a predefined grid. **3) Adaptability:** Existing fairness methods cannot be directly used for deepfake detection scenarios (see details in Section 3.2). We propose a learning objective in DAW-FDD, which is adaptable to existing fairness objectives and easily integrates into different deepfake detectors.

We demonstrate the fairness and effectiveness of our methods using large-scale datasets (FaceForensics++ [50], Celeb-DF [33], DeepFakeDetection (DFD) [1], and Deepfake Detection Challenge (DFDC) [9]). The main contributions of our work can be summarized as follows:

1. We present the first study of methods that can alleviate the lack of fairness in deepfake detection.
2. We describe two methods for achieving fair deepfake detection (FDD) in ways that are agnostic or aware of demographic factors of data.
3. We propose convex learning objectives expressed in terms of individual sample loss or subgroup loss based on CVaR, which is easier to optimize.
4. Empirical experiments on several benchmark datasets confirm the effectiveness of our method in improving the fairness of state-of-the-art deepfake detectors.

2. Related Work

2.1. The Categories of Fairness Approaches

Several approaches have been proposed to improve fairness in general machine learning settings. These methods fall into two major categories: demographic-agnostic and demographic-aware.

Demographic-agnostic. When demographic information

Method	Year	#Detector	#Dataset	Fairness Solution	Require Demographics
Trinh <i>et al.</i> [53]	2021	3	1	×	-
Hazirbas <i>et al.</i> [21]	2021	5	1	×	-
Pu <i>et al.</i> [44]	2022	1	1	×	-
GBDF [40]	2022	5	4	Data-level	✓
Xu <i>et al.</i> [62]	2022	3	4	×	-
DAG-FDD (ours)	2023	5	4	Algorithm-level	×
DAW-FDD (ours)	2023	5	4	Algorithm-level	✓

Table 1. Summary of previous studies and our work. ‘-’ means not applicable.

is inaccessible, methods to achieve fairness without any prior knowledge of the sensitive attributes have emerged. These approaches are inspired by the Rawlsian Maximin principle [47] such as the distributionally robust optimization (DRO)-based approach [20] and adversarial learning-based approach [30]. Other approaches such as using input features to find surrogate subgroup information [67], cluster-based balancing strategy for input data [63], through knowledge distillation [5], and via causal variational autoencoder [17] are also proposed. However, these approaches usually may raise a high degradation on the model’s accuracy performance.

Demographic-aware. A larger number of fairness definitions have been proposed in the literature for generating penalties for learning loss. To sum up, there are two types of fairness measures using demographics: group fairness [13] and intersectional fairness [15]. Specifically, group fairness considers a model fair across a user-specified set of subgroups if these different subgroups have similar predicted outcomes. Intersectional fairness considers a notion of intersectional fairness that accounts for multiple sensitive attributes. Many related popular fairness constraints are designed such as demographic parity [35] and Equal Odds [18]. We only list a few of them. More fairness constraints with using demographics can be found in [4, 38]. These constraint-based approaches have a common drawback, which is resulting in non-convex learning objectives. Furthermore, these specified methods of fairness can only constrain the model to achieve fairness in specific aspects.

2.2. Fairness in Deepfake Detection

Despite great efforts [10, 11, 37, 59, 66] being dedicated to enhancing the generalization capability of deepfake detection over out-of-distribution (OOD) data, there is still limited progress in addressing the biased performance during testing within known domains. In contrast to previous studies, our research uniquely prioritizes fairness as its primary goal. Specifically, we address the issue of biased performance among subgroups under in-domain testing, aiming to achieve equal treatment and accuracy for all demographic subgroups.

Extending the investigation of fairness originated for face recognition [14, 25, 46, 64], several recent studies have examined fairness concerns in deepfake detection, as shown in Table 1. The work in [53] is the first to evaluate biases

in existing deepfake datasets and detection models across protected subgroups. They examined three popular deepfake detectors and observed large disparities in predictive performances across races, with up to 10.7% difference in error rate among subgroups. Similar observations are found in [21]. Pu *et al.* [44] evaluated the reliability of one popular deepfake detection model (MesoInception-4) on FF++ and showed that the MesoInception-4 model is generally more effective for female subjects. A more comprehensive analysis of deepfake detection bias with regards to demographic and non-demographic attributes is presented in [62]. The authors added massive and diverse annotations for 5 widely-used deepfake detection datasets to facilitate future research. The work in [40] showed significant bias in both datasets and detection models and they tried to reduce the performance bias across genders by providing a gender-balanced dataset. This leads to limited improvement at the cost of highly time-consuming data annotation, which can hardly handle the fairness towards different attributes. Therefore, developing more effective bias-mitigating deepfakes detection solutions is in high demand [36].

3. Method

In this work, we aim to develop method that can build fairness considerations directly in the deep learning based deepfake detection models. To this end, we propose two methods based on the notion of *Conditional-Value-at-Risk* (CVaR). The first method, termed DAG-FDD, is applicable when we have training data without demographic annotations, in which case it can work with most existing deepfake dataset. The second method, termed DAW-FDD, works when the dataset contains additional demographic annotations. This method takes into account fairness, accuracy, and robustness simultaneously to address the imbalanced nature of the data.

3.1. Demographic-agnostic FDD (DAG-FDD)

We propose the DAG-FDD method that improves fairness in deepfake detection without using latent attributes, based on the distributionally robust optimization (DRO) principles [12, 20].

Problem setup. Let $\mathcal{S} = \{(X_i, Y_i)\}_{i=1}^n$ be a training dataset with a joint distribution \mathbb{P} , where X_i represents data feature and Y_i is the corresponding label. Suppose there are K subgroups that comprise \mathbb{P} . Therefore, we can represent \mathbb{P} as a mixture of K distributions $\mathbb{P} := \sum_{m=1}^K \pi_m \mathbb{P}_m$, where the m -th subgroup has an occurrence probability $\pi_m \in (0, 1)$ and a distribution \mathbb{P}_m . Moreover, $\sum_{m=1}^K \pi_m = 1$ and the smallest minority subgroup has the smallest value of π_m . We seek to minimize the following worst-case risk:

$$\mathcal{R}_{\max}(\theta) := \max_{m=1, \dots, K} \mathbb{E}_{(X, Y) \sim \mathbb{P}_m} [\ell(\theta; X, Y)], \quad (1)$$

where ℓ is a loss function (e.g., cross-entropy loss) that depends on the model parameters θ and data point (X, Y) .

Algorithm 1: DAG-FDD

Input: A training dataset \mathcal{S} of size n , α , max_iterations, num_batch, learning rate η
Output: A fair deepfake detection model with parameters θ^*

```

1 Initialization:  $\theta_0, l = 0$ 
2 for  $e = 1$  to max_iterations do
3   for  $b = 1$  to num_batch do
4     Sample a mini-batch  $\mathcal{S}_b$  from  $\mathcal{S}$ 
5     Compute  $\ell(\theta_l; X_i, Y_i), \forall (X_i, Y_i) \in \mathcal{S}_b$ 
6     Using binary search to find  $\lambda$  that minimizes (2) on  $\mathcal{S}_b$ 
7     Compute  $\theta_{l+1}$  with equation (3)
8      $l \leftarrow l + 1$ 
9   end
10 end
11 return  $\theta^* \leftarrow \theta_l$ 

```

Directly minimizing \mathcal{R}_{\max} is intractable since we have no information about the latent sensitive subgroups (i.e., \mathbb{P}_m) nor the total number of subgroups (i.e., K). However, we can solve an empirical version of its upper bound.

Upper bound of $\mathcal{R}_{\max}(\theta)$. We explore the well-known *Conditional Value-at-Risk* (CVaR) [48],

$$\text{CVaR}_{\alpha}(\theta) := \inf_{\lambda \in \mathbb{R}} \left\{ \lambda + \frac{1}{\alpha} \mathbb{E}_{(X, Y) \sim \mathbb{P}} [\ell(\theta; X, Y) - \lambda]_+ \right\},$$

where $[a]_+ = \max\{0, a\}$ is the hinge function and $\alpha \in (0, 1)$ is a hyperparameter. The following result shows that the risk $\text{CVaR}_{\alpha}(\theta)$ is an upper bound of $\mathcal{R}_{\max}(\theta)$, so that we can optimize it to achieve a low worst-case risk.

Proposition 1. Let a lower bound $\alpha \leq \min_{m=1, \dots, K} \pi_m$. Then $\text{CVaR}_{\alpha}(\theta) \geq \mathcal{R}_{\max}(\theta)$.

Note that this result is not new [65]. However, we are the first to apply it in designing fairness losses for learning fair deepfake detectors in a demographic-agnostic way. We include the proof of proposition 1 in Appendix A.1. In practice, α is a user-predefined hyperparameter since we do not know $\{\pi_m\}_{m=1}^K$ nor K . Choosing α to be smaller indicates that we want to ensure subgroups with smaller probabilities also have a low expected loss.

DAG-FDD. Therefore, we can minimize an empirical version of $\text{CVaR}_{\alpha}(\theta)$ based on the previous discussion. This gives us the following optimization problem:

$$\min_{\theta, \lambda \in \mathbb{R}} \mathcal{L}_{\text{DAG-FDD}}(\theta, \lambda) := \lambda + \frac{1}{\alpha n} \sum_{i=1}^n [\ell(\theta; X_i, Y_i) - \lambda]_+. \quad (2)$$

After obtaining the optimal value of λ^* in (2), we only consider samples with losses above λ^* for learning a FDD. We call this method DAG-FDD. Solving the optimization problem in (2) can be done through an iterative gradient descent approach [23]. In practice, we first initialize the model parameters θ and then randomly select a mini-batch set \mathcal{S}_b from the training set \mathcal{S} , performing the following two steps for each iteration on \mathcal{S}_b (see Algorithm 1):

- We fix θ and use binary search to find the global optimum of λ since $\mathcal{L}_{\text{DAG-FDD}}(\theta, \lambda)$ is convex w.r.t. λ .
- We fix λ and update θ using (stochastic) gradient descent:

$$\theta_{l+1} = \theta_l - \frac{\eta}{\alpha|\mathcal{S}_b|} \sum_{i \in \mathcal{S}_b} \partial_{\theta} \ell(\theta_l; X_i, Y_i) \cdot \mathbb{I}_{[\ell(\theta_l; X_i, Y_i) > \lambda]}, \quad (3)$$

where $\mathbb{I}_{[a]}$ is an indicator function that equals 1 if a is true, and 0 otherwise. $\partial_{\theta} \ell$ represents the (sub)gradient of ℓ w.r.t. θ , and η is the learning rate.

We stop iterating after user-specified stopping criteria is reached (e.g., the maximum number of iterations reached). Note that our optimization process is similar to the standard training process of deepfake models, but with an additional binary search to find λ , and therefore has a time complexity comparable to them.

3.2. Demographic-aware FDD (DAW-FDD)

Creating a demographic information-based deepfake detection dataset can be a laborious task that requires extensive data labeling. However, recent efforts have produced useful datasets, such as the gender-balanced deepfake dataset provided by [40] and the large-scale attribute annotations for several popular deepfake datasets provided by [62]. To introduce fairness, a common approach is to include a fairness penalty in the learning objective. This method is known as the constraint-based fairness approach and has gained popularity in recent years.

However, this approach has two drawbacks. First, the non-convexity of the fairness penalty makes the learning objective non-convex. Second, fairness is only guaranteed on one specific measure, such as demographic parity [13] or equalized odds [18], limiting the scalability and applicability of the designed deepfake detection models on different datasets. Additionally, due to the imbalanced nature of the deepfake dataset, it is important to address the issue of imbalanced data when designing fair detection models. To address these issues, we propose DAW-FDD, a method for modeling fair deepfake detection models using available demographic information.

Problem setup. We consider a set of user-specified subgroups, denoted as \mathcal{G} . Each subgroup, represented by $g \in \mathcal{G}$, has its subgroup risk defined as $L_g(\theta) := \mathbb{E}_{(X,Y)|G=g}[\ell(\theta; X, Y)]$, where G denotes the demographic variable of X . We introduce a random variable $\mathbb{L}(\theta)$, which selects from the set of subgroup risks $\{L_g(\theta)\}_{g \in \mathcal{G}}$. Our objective is to minimize the following risk:

$$\mathcal{R}(\mathbb{L}(\theta)) := \mathbb{E}[\mathbb{L}(\theta)] + \mathbb{D}[\mathbb{L}(\theta)], \quad (4)$$

Here, $\mathbb{E}[\mathbb{L}(\theta)]$ represents the average subgroup risk, and $\mathbb{D}[\mathbb{L}(\theta)]$ quantifies the deviation within $\mathbb{L}(\theta)$. The goal of (4) is to minimize all subgroup risks while maintaining their similarity. However, using this approach to create a loss function for fair model learning faces two challenges. First,

selecting an appropriate deviation measure \mathbb{D} can be difficult. Second, this method can lead to non-convex loss functions due to the non-convex nature of deviation measures, potentially resulting in suboptimal local solutions. Fortunately, these challenges can be overcome by replacing this approach with a fairness risk measure, as suggested in [61].

Fairness risk measure. For $\alpha \in (0, 1)$, we define $\mathcal{R}(\mathbb{L}(\theta)) := \text{CVaR}_{\alpha}(\mathbb{L}(\theta)) = \inf_{\lambda \in \mathbb{R}} \{\lambda + \frac{1}{\alpha} \mathbb{E}[(\mathbb{L}(\theta) - \lambda)_+]\}$ and $\mathbb{D}[\mathbb{L}(\theta)] := \text{CVaR}_{\alpha}(\mathbb{L}(\theta) - \mathbb{E}[\mathbb{L}(\theta)])$. Note that $\text{CVaR}_{\alpha}(\cdot)$ has a similar formula as it in Section 3.1. However, they have different meanings. Specifically, in Section 3.1, $\text{CVaR}_{\alpha}(\cdot)$ is applied to individual losses of sample. Here, it is applied to all subgroup risks. In addition, $\text{CVaR}_{\alpha}(\mathbb{L}(\theta) - \mathbb{E}[\mathbb{L}(\theta)])$ measures the deviation of $\mathbb{L}(\theta)$ above its mean. In [61], $\text{CVaR}_{\alpha}(\mathbb{L}(\theta))$ is considered a fairness risk measure based on the following result:

Proposition 2. (equation (21) of [61]) Let $\alpha \in (0, 1)$,

$$\min_{\theta} \text{CVaR}_{\alpha}(\mathbb{L}(\theta)) = \min_{\theta} \mathbb{E}[\mathbb{L}(\theta)] + \mathbb{D}[\mathbb{L}(\theta)].$$

Similarly, α is a user-specified hyperparameter. From this proposition, we can clearly find that optimizing $\text{CVaR}_{\alpha}(\mathbb{L}(\theta))$ can directly achieve accuracy and fairness for a model instead of using (4). Most importantly, $\text{CVaR}_{\alpha}(\mathbb{L}(\theta))$ is convex, which can provide more opportunities to avoid bad local optima solutions during model training.

In deepfake detection, using the empirical version of $\text{CVaR}_{\alpha}(\mathbb{L}(\theta))$ may not be effective for learning FDD models because it relies on accurate estimation of subgroup risks. In practice, for each subgroup, $L_g(\theta)$ is usually estimated and approximated by using the average operator on all individual losses of examples from that subgroup. However, imbalanced classes (fake and real) in most deepfake datasets often cause a high-tail phenomenon in each subgroup, which requires fair models with good tail performance that perform well across both classes instead of just on average. To address this, we propose a DAW-FDD approach that uses the average top- k operator [34] to estimate subgroup risks instead of the average operator as follows:

DAW-FDD. Let $\ell^{g_i}(\theta) := \{\ell(\theta; X_j, Y_j)\}_{j: G_j = g_i}$ be the set of individual losses on the training examples that have demographic feature $g_i \in \mathcal{G}$ with size $|g_i|$. Denote $\ell_{[j]}^{g_i}(\theta)$ as the j -th largest loss in $\ell^{g_i}(\theta)$ (ties can be broken in any consistent way). For integers $1 \leq k_i \leq |g_i|$, where k_i may vary for different subgroups, we define the following optimization problem:

$$\min_{\theta, \lambda \in \mathbb{R}} \lambda + \frac{1}{\alpha|\mathcal{G}|} \sum_{i=1}^{|\mathcal{G}|} [L_i(\theta) - \lambda]_+, \text{ s.t. } L_i(\theta) = \frac{1}{k_i} \sum_{j=1}^{k_i} \ell_{[j]}^{g_i}(\theta), \quad (5)$$

where $|\mathcal{G}|$ is the size of \mathcal{G} . Here, $\mathcal{G} = \{g_1, \dots, g_{|\mathcal{G}|}\}$. In the above formula, we use the average top k_i individual

Algorithm 2: DAW-FDD

Input: A training dataset \mathcal{S} with demographic variable \mathcal{G} , A set of subgroups \mathcal{G} , α , α_i , max_iterations, num_batch, η
Output: A fair deepfake detection model with parameters θ^*

```

1 Initialization:  $\theta_0, l = 0$ 
2 for  $e = 1$  to max_iterations do
3   for  $b = 1$  to num_batch do
4     Sample a mini-batch  $\mathcal{S}_b$  from  $\mathcal{S}$ 
5     Compute  $\ell(\theta_l; X_j, Y_j), \forall (X_j, Y_j) \in \mathcal{S}_b$ 
6     For each  $i \in \{1, \dots, |\mathcal{G}|\}$ , set  $\lambda_i^*$  to be the value of  $\lambda_i$ 
       that minimizes  $L_i(\theta, \lambda_i)$  as given in (6b). This
       minimization is solved using binary search.
7     Set  $L_i(\theta) \leftarrow L_i(\theta, \lambda_i^*)$  using (6b),  $\forall i$ 
8     Using binary search to find  $\lambda$  that minimizes (6a)
9     Set  $\theta_{l+1} \leftarrow \theta_l - \eta \partial_\theta \mathcal{L}_{\text{DAW-FDD}}(\theta_l, \lambda)$ 
10     $l \leftarrow l + 1$ 
11  end
12 end
13 return  $\theta^* \leftarrow \theta_l$ 

```

losses in $\ell^{g_i}(\theta)$ (i.e., $L_i(\theta)$) to approximate the subgroup g_i 's risk $L_{g_i}(\theta)$. This will enhance the effect of the minority class and reduce the influence of the majority class in each subgroup, as samples with small loss values are most likely from the majority class in the training set. Since k_i may vary across subgroups, we set $k_i = \alpha_i |g_i|$, where $\alpha_i \in [1/|g_i|, 1]$. Therefore, in practice, we can set a uniform α_i for all subgroups and tune it on a predefined grid.

The ranking operation in the constraint of (5) is the main obstacle to using it as a learning objective in an efficient way. However, we can substitute the ranking operation with a minimization problem by using the following result (the proof can be found in Appendix A.2).

Theorem 1. For a set of real numbers $\bar{\ell} = \{\ell_1, \dots, \ell_n\}$, $\ell_{[k]}$ is the k -th largest value in $\bar{\ell}$, and an integer $k \in [1, n]$, we have $\frac{1}{k} \sum_{i=1}^k \ell_{[i]} = \min_{\lambda \in \mathbb{R}} \lambda + \frac{1}{k} \sum_{i=1}^n [\ell_i - \lambda]_+$. Let $k_i = \alpha_i |g_i|$, then equation (5) is equivalent to

$$\min_{\theta, \lambda \in \mathbb{R}} \mathcal{L}_{\text{DAW-FDD}}(\theta, \lambda) := \lambda + \frac{1}{\alpha |\mathcal{G}|} \sum_{i=1}^{|\mathcal{G}|} [L_i(\theta) - \lambda]_+, \quad (6a)$$

$$\text{s.t. } L_i(\theta) = \min_{\lambda_i \in \mathbb{R}} L_i(\theta, \lambda_i) := \lambda_i + \frac{1}{\alpha_i |g_i|} \sum_{j: S_j = g_i} [\ell(\theta; X_j, Y_j) - \lambda_i]_+. \quad (6b)$$

Theorem 1 tells us that we can replace the average top- k loss in each subgroup with a CVaR loss with auxiliary parameter λ_i . It is clear that two CVaR formulas are in the optimization problem (6). However, they possess distinct meanings. The outer CVaR fosters fairness across different subgroups, promoting *inter-subgroup* equity and model accuracy, while the inner CVaR promotes fairness across both real and fake examples within the same subgroup, improving *intra-subgroup* equity and model robustness. We call this approach DAW-FDD. To optimize (6), the iterative optimization procedure in Algorithm 1 can still be applied

except where each iteration now consists of three steps: updating λ^i , λ , and θ . The pseudocode is shown in Algorithm 2. Note that the explicit form of $\partial_\theta \mathcal{L}_{\text{DAW-FDD}}(\theta_l, \lambda)$ (i.e., the (sub)gradient of $\mathcal{L}_{\text{DAW-FDD}}(\theta, \lambda)$ w.r.t. θ) can be found in Appendix B.

Remark 1. Our DAW-FDD method can generalize several existing fairness methods by adjusting the values of α and α_i . For example, if $\alpha \rightarrow 1$ and $\alpha_i \rightarrow 1$, it becomes the minimization of average subgroup risks, which aligns with the impartial observer principle [19]. In addition, it becomes the minimization of the largest subgroup risk (1) [20, 39] if $\alpha \rightarrow 0$ and $\alpha_i \rightarrow 1$, which aligns with the maximin principle [47]. If $\alpha_i \rightarrow 1$, our approach is just the empirical version of fairness risk measure $\text{CVaR}_\alpha(\mathbb{L}(\theta))$ [61]. It is obvious that our method is more scalable and flexible.

4. Experiment

This section evaluates the effectiveness of the proposed methods in terms of fairness performance and deepfake detection performance. We present the most significant information and results of our experiments. More detailed information, additional results, and codes are provided in Appendix C, D, and supplementary files, respectively.

4.1. Experimental Settings

Datasets. Our experiments are based on four popular large-scale benchmark deepfake datasets, namely FaceForensics++ (FF++) [50], Celeb-DF [33], DeepFakeDetection (DFD) [1], and Deepfake Detection Challenge Dataset (DFDC) [9]. Since all the original datasets do not have the demographic information of each video or image, we use the annotations from [62] which provides massively annotated data for these four datasets, including Gender (Male and Female) and Race (Asian, White, Black, and Others) attributes. We also double-check the annotations for each dataset. In addition to the single attribute fairness, we also consider the combined attributes (Intersection) group, including Male-Asian (M-A), Male-White (M-W), Male-Black (M-B), Male-Others (M-O), Female-Asian (F-A), Female-White (F-W), Female-Black (F-B), and Female-Others (F-O). We use Dlib [28] for face extraction and alignment, and the cropped faces are resized to 380×380 for training and testing. Following the previous study [62], we split the annotated datasets into training/validation/test sets with a ratio of approximately 60%/20%/20%, without identity overlapping. In particular, the validation set is used for hyperparameter tuning. More details of the datasets, including attribute groups and number of training samples are provided in the Table D.5 and D.6 of the Appendix D.7.

Evaluation Metrics. Fairness measures are selected considering the practical use of deepfake detection systems on social media platform. Given the real cases outnumber fake

Methods	Require Demographics	Fairness Metrics (%) ↓									Detection Metrics (%)			
		Gender			Race			Intersection			Overall			
		G_{FPR}	F_{FPR}	F_{EO}	G_{FPR}	F_{FPR}	F_{EO}	G_{FPR}	F_{FPR}	F_{EO}	AUC ↑	FPR ↓	TPR ↑	ACC ↑
Original	—	4.10	4.10	9.06	13.09	17.28	21.00	17.93	31.59	53.95	92.76	22.06	94.43	91.49
DRO $_{\chi^2}$ [20]	×	2.68	2.68	6.75	8.32	8.97	20.40	8.73	22.97	55.54	97.18	6.32	90.25	90.86
DAG-FDD (Ours)		1.63	1.63	6.21	8.23	9.53	11.49	9.65	21.21	48.10	97.13	9.54	94.32	93.63
Naive [40]	✓	11.98	11.98	18.20	16.57	22.01	25.97	28.90	72.19	93.59	83.17	50.77	92.62	84.87
FRM [61]		1.33	1.33	5.88	9.24	12.75	20.13	10.39	25.57	60.90	97.81	4.76	90.85	91.63
Group DRO [51]		8.20	8.20	12.87	14.37	20.97	23.79	21.86	44.98	65.24	91.13	27.83	95.15	91.04
Cons. EFPR [56]		4.24	4.24	7.91	7.09	7.49	12.41	14.95	27.80	46.62	94.30	22.61	94.94	91.80
Cons. EO [56]		1.77	1.77	4.79	10.92	12.61	16.50	17.25	26.95	44.68	95.74	16.28	95.89	93.72
DAW-FDD (Ours)		0.32	0.32	3.99	2.49	3.88	6.29	6.61	14.06	33.84	97.46	11.46	95.40	94.17

Table 2. Comparison results with different fairness solutions using Xception detector on FF++ testing set across Gender, Race, and Intersection groups. The best results are shown in **Bold**. ↑ means higher is better and ↓ means lower is better. Gray highlights mean our methods outperform the baselines in the group (i.e., DAG-FDD vs. Original/DRO $_{\chi^2}$, DAW-FDD vs. Original/Naive/FRM/Group DRO/Cons. EFPR/Cons. EO).

ones, we prioritized metrics related to False Positives (misclassifying real as fake) to prevent potential consequences such as suspicion, distrust, legal, or social repercussions, especially for users from specific ethnic groups. Three fairness metrics are used to report the fairness performance of methods. Specifically, we report the maximum differences in False Positive Rate (FPR) Gap (G_{FPR}) for Gender, Race, and Intersection groups. We also consider the Equal False Positive Rate (F_{FPR}) and Equal Odds (F_{EO}) metrics as used in [56]. These metrics are defined as follows:

$$\begin{aligned}
G_{FPR} &= \max_{g, g' \in \mathcal{G}} |FPR_g - FPR_{g'}|, \\
F_{FPR} &:= \sum_{g \in \mathcal{G}} \left| \frac{\sum_{i=1}^n \mathbb{I}[\hat{Y}_i=1, G_i=g, Y_i=0]}{\sum_{i=1}^n \mathbb{I}[G_i=g, Y_i=0]} - \frac{\sum_{i=1}^n \mathbb{I}[\hat{Y}_i=1, Y_i=0]}{\sum_{i=1}^n \mathbb{I}[Y_i=0]} \right|, \\
F_{EO} &:= \sum_{g \in \mathcal{G}} \sum_{q=0}^1 \left| \frac{\sum_{i=1}^n \mathbb{I}[\hat{Y}_i=1, G_i=g, Y_i=q]}{\sum_{i=1}^n \mathbb{I}[G_i=g, Y_i=q]} - \frac{\sum_{i=1}^n \mathbb{I}[\hat{Y}_i=1, Y_i=q]}{\sum_{i=1}^n \mathbb{I}[Y_i=q]} \right|, \quad (7)
\end{aligned}$$

where FPR_g represents the FPR scores of subgroup g . We assume a test set comprising indices $\{1, \dots, n\}$. Y_i and \hat{Y}_i respectively represent the true and predicted labels of the sample X_i . Their values are binary, where 0 means real and 1 means fake. For all fairness metrics, a lower value means better performance.

Since there is usually a trade-off between fairness and detection performance [4, 38], we also include detection metrics to assess the balance between fairness and detection performance. Four widely-used deepfake detection metrics are reported: 1) the area under the curve (AUC), 2) FPR, which is essential in real-world use as it indicates the count of incorrect fake classifications, 3) True Positive Rate (TPR), which measures the number of correct fake classification, and 4) Accuracy (ACC). We calculate the FPR, TPR, and ACC with a fixed threshold of 0.5 [7, 58].

Baseline Methods. We apply the two types of loss functions proposed in Section 3 to popular deepfake detectors to show their effectiveness. Five deepfake detection models are considered, including three widely-used CNN architectures in deepfake detection [33, 40, 41] (i.e., Xception [50], ResNet-50 [22], and EfficientNet-B3 [52]) and two well-

Methods	Fairness Metrics (%) ↓			Detection Metrics (%)				Training Time (mins)/Epoch	Binary Search Time (mins)/Epoch
	G_{FPR}	F_{FPR}	F_{EO}	AUC ↑	FPR ↓	TPR ↑	ACC ↑		
Original	24.00 (9.00)	45.50 (16.39)	63.24 (12.96)	95.00 (2.96)	19.28 (7.14)	95.94 (1.41)	93.29 (1.60)	2.6	N/A
DAG-FDD (Ours)	13.83 (11.86)	24.38 (17.04)	48.52 (15.37)	96.81 (1.68)	13.43 (7.00)	95.33 (1.40)	93.81 (1.13)	3.0	0.59
DAW-FDD (Ours)	11.53 (3.43)	26.55 (7.97)	47.50 (10.99)	97.40 (0.30)	12.21 (4.05)	95.45 (1.37)	94.11 (0.66)	3.0	0.66

Table 3. Detection mean and standard deviation (in parentheses) of Xception detector on FF++ testing set across 5 experimental repeats, in the same format as Table 2. Training time and binary search time per epoch for each method are also reported.

designed deepfake detectors with outstanding performance, namely DSP-FWA [33] and RECCE [3]. We denote the detectors with their original loss functions (e.g., binary cross-entropy) as “Original”.

In terms of comparison in fairness detection, we consider the method [40] based on balancing the number of training samples in each subgroup for deepfake fairness improvement. Despite we have discussed the drawbacks of this strategy in Section 1, we take this method as a baseline for comparison, noted as “Naive”. Specifically, we use an intersectional subgroup with the smallest number of training samples and then randomly select the same number of training samples from the other subgroups to create such a balanced training dataset. Moreover, we compare our two loss functions with the χ^2 -divergence based DRO (DRO $_{\chi^2}$) [20], the fairness risk measure (FRM) [61], and a popular Group DRO method [51] in fairness research although they have not been applied to deepfake detection. Besides, we modify F_{FPR} and F_{EO} as regularization terms [56], and incorporate them with binary cross-entropy loss as baselines: Cons. EFPR and Cons. EO.

Implementation Details. All experiments are conducted on the PyTorch platform [43] using 4 NVIDIA RTX A6000 GPU cards. We train all methods by using a (mini-batch) stochastic gradient descent optimizer with batch size 640, epochs 200, and learning rate as 5×10^{-4} . We build our loss functions on the binary cross-entropy loss for the binary deepfake classification task. Since the DAW-FDD method needs to pre-define a set of subgroups, we use the Intersection group in experiments and also report the performance on single attributes. The hyperparameters α and α_i are

Datasets	Methods	Fairness Metrics (%) ↓									Detection Metrics (%)			
		Gender			Race			Intersection			Overall			
		G_{FPR}	F_{FPR}	F_{EO}	G_{FPR}	F_{FPR}	F_{EO}	G_{FPR}	F_{FPR}	F_{EO}	AUC ↑	FPR ↓	TPR ↑	ACC ↑
Celeb-DF	Original	4.93	4.93	22.04	3.31	4.77	26.06	11.81	15.66	39.95	97.17	13.01	95.83	94.05
	DAG-FDD (Ours)	2.02	2.02	16.77	1.20	1.22	28.56	2.54	3.09	30.43	98.00	2.42	87.40	89.44
	DAW-FDD (Ours)	3.81	3.81	18.93	3.14	3.34	33.91	3.80	4.91	35.48	98.03	2.10	84.53	87.21
DFD	Original	2.95	2.95	5.52	7.35	7.35	7.72	8.67	15.81	24.31	92.94	25.00	96.01	89.09
	DAG-FDD (Ours)	2.92	2.92	4.79	6.08	6.08	7.05	8.30	13.52	19.57	93.40	28.07	96.31	88.28
	DAW-FDD (Ours)	1.40	1.40	3.14	2.36	2.36	3.35	7.20	8.74	14.70	93.17	27.75	95.95	88.14
DFDC	Original	1.64	1.64	4.36	4.02	5.85	38.84	20.17	38.68	119.71	92.40	7.28	76.32	86.87
	DAG-FDD (Ours)	1.30	1.30	5.38	4.50	5.78	46.56	14.65	33.79	113.93	92.69	6.61	74.41	86.61
	DAW-FDD (Ours)	1.73	1.73	3.39	3.48	4.14	42.87	11.19	23.63	115.15	94.88	4.27	75.10	88.37

Table 4. Results of Xception detector on Celeb-DF, DFD, and DFDC testing sets, in the same format as Table 2.

Models	Methods	Fairness Metrics (%) ↓									Detection Metrics (%)			
		Gender			Race			Intersection			Overall			
		G_{FPR}	F_{FPR}	F_{EO}	G_{FPR}	F_{FPR}	F_{EO}	G_{FPR}	F_{FPR}	F_{EO}	AUC ↑	FPR ↓	TPR ↑	ACC ↑
ResNet-50	Original	2.58	2.58	6.64	12.80	15.45	17.62	20.06	43.18	60.66	94.32	25.96	96.36	92.37
	DAG-FDD (Ours)	2.21	2.21	6.37	6.44	11.42	14.17	16.68	37.50	52.79	94.51	22.52	95.34	92.15
	DAW-FDD (Ours)	3.78	3.78	10.21	7.01	8.27	13.09	13.28	35.08	60.07	93.70	23.56	93.65	90.58
EfficientNet-B3	Original	1.97	1.97	4.15	9.05	10.86	14.12	13.38	22.65	40.13	95.91	20.25	97.21	94.09
	DAG-FDD (Ours)	0.47	0.47	5.36	9.48	9.58	13.50	10.87	19.34	46.08	97.20	8.40	92.87	92.65
	DAW-FDD (Ours)	0.04	0.04	5.53	3.79	4.67	12.63	6.43	12.57	43.72	96.30	8.22	91.43	91.49
DSP-FWA	Original	5.90	5.90	11.81	11.07	14.58	21.98	21.38	48.20	75.91	91.79	31.64	93.17	88.74
	DAG-FDD (Ours)	4.64	4.64	9.77	12.52	18.04	25.03	15.61	40.57	74.54	91.47	32.35	93.70	89.05
	DAW-FDD (Ours)	3.02	3.02	11.30	5.75	10.52	19.34	12.84	36.05	75.73	90.84	30.43	91.97	87.97
RECCE	Original	0.87	0.87	3.14	18.81	27.65	30.07	30.26	67.38	80.34	98.05	21.20	98.21	94.74
	DAG-FDD (Ours)	0.55	0.55	3.71	12.68	17.41	20.33	15.40	36.17	54.24	98.33	12.01	96.80	95.23
	DAW-FDD (Ours)	0.25	0.25	4.75	6.99	7.96	11.95	13.54	23.44	52.95	98.35	8.15	94.59	94.10

Table 5. Results of ResNet-50, EfficientNet-B3, DSP-FWA, and RECCE detectors on FF++ testing set, in the same format as Table 2.

tuned on the grid $\{0.1, 0.3, 0.5, 0.7, 0.9\}$. Following [26], the final hyperparameter setting per dataset and per method is determined based on a preset rule that allows up to a 5% degradation of overall AUC in the validation set from the corresponding ‘‘Original’’ method while minimizing the intersectional F_{FPR} . More details and the evaluation of the influence of different parameter settings on detection performance are provided in Appendix C.2, D.2.

4.2. Results

Performance on FF++ Dataset. We first report the comparison results of our methods with several baselines on the FF++ dataset using the Xception deepfake detector. The results are shown in Table 2. The results show that in the cases where demographic information is unavailable from the training data, our DAG-FDD method achieves superior fairness performance to the Original method across most metrics for all three sensitive attribute groups, as shown in gray highlights. For example, we enhance the G_{FPR} of Gender, F_{EO} of Race, and F_{FPR} of Intersection by 2.47%, 9.51%, and 10.38%, respectively, compared to the Original. These results indicate our method has strong applicability in scenarios where demographic data is unavailable. In addition, it is clear that our method outperforms the DRO_{χ^2} method on most fairness metrics. This is benefited from the tighter upper bound (see Proposition 1) on the risk $\mathcal{R}_{\max}(\theta)$ in our DAG-FDD method than the DRO_{χ^2} method as mentioned in [65].

With demographic information, it can be observed that the Naive method trained on a balanced dataset does not guarantee an improvement in both in the fairness of test-

ing results. For example, on the intersectional subgroups, all fairness performances of the Naive method (e.g., F_{FPR} : 72.19%) are worse than the Original method (e.g., F_{FPR} : 31.59%). This can be attributed to the fact that a naive balancing strategy will reduce the number of available training samples, resulting in a significant decrease in detection performance. The same trends can be found in AUC scores, which decrease from 92.76% (Original) to 83.17% (Naive), and in FPR scores, which increase from 22.06% (Original) to 50.77% (Naive). Therefore, a poorly trained model may lead to unfairness.

In addition, our DAW-FDD method outperforms all methods on the most fairness metrics (as shown in Bold). The reason is that DAW-FDD uses the additional demographic information to guide the detector training to achieve fairness without reducing the dataset size. In particular, the DAW-FDD method achieves the best fairness performance on all metrics in the Intersection group thanks to the guidance of intersection group information in the design of DAW-FDD. The superiority of DAW-FDD over Group DRO is evident. Specifically, Group DRO do not show any improvement, possibly because it places greater emphasis on improving the worst-subgroup generalization performance and less on ensuring overall fairness. Furthermore, in our comparison between the DAW-FDD and FRM methods, we have found our method outperforms FRM. This result clearly demonstrates the effectiveness of our robust learning strategy, which operates at the sample level within each subgroup, in enhancing fairness.

Most importantly, our DAG-FDD and DAW-FDD methods not only enhance fairness performance but also improve

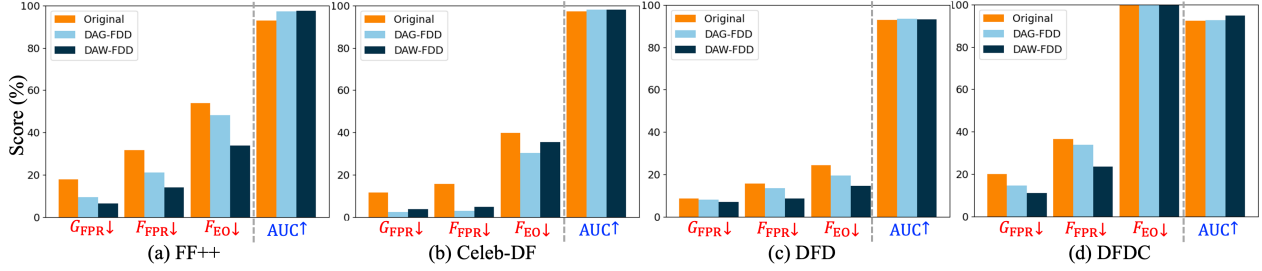


Figure 1. Comparison of Xception detector on Intersection group of four datasets: (a) FF++, (b) DFDC, (c) DFD, and (d) DFDC.

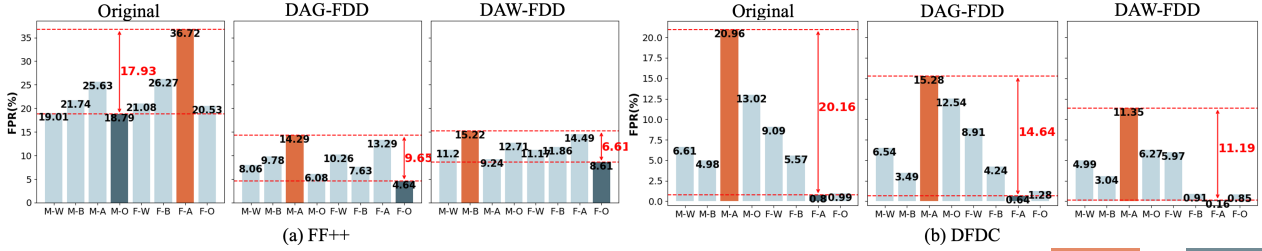


Figure 2. FPR comparison of Xception detector on intersectional subgroups of (a) FF++ and (b) DFDC dataset. Orange and dark cyan bars show the subgroups with the highest and lowest FPR, respectively, while the double arrow indicates their gap (smaller is better).

the detection performance of the detector. For example, we improve an approximately 4.7% in AUC and 12.52% in FPR when compared with the Original method. The stability evaluation results of our methods with 5 random runs are shown in Table 3. It is clear that our methods demonstrate a robust and formidable capacity to improve fairness. This is likely due to our methods being designed on CVaR, which is a DRO method that can improve model performance [12]. We also show the training time per epoch costs during training Xception on FF++ dataset in Table 3. Based on the presented table results, our methods show a slightly higher time requirement compared to the original method. However, the difference is minimal, mainly due to the incorporation of a binary search in the calculation of model training loss.

Performance on Different Datasets. Table 4 shows the evaluation performance of the Xception detector on three popular deepfake datasets. It is clear that our proposed DAG-FDD and DAW-FDD methods outperform the Original method on all three datasets across all groups and most fairness metrics, especially on the Intersection group (also as shown in Figure 1). In the meantime, our methods achieve similar or even better performances on most detection metrics. Note that our methods on the Celeb-DF dataset lead to a decrease in TPR. One possible reason is that our methods involve hyperparameter tuning based on F_{FPR} , as mentioned in experimental settings. To evaluate the effectiveness of our method to other metrics, we employ F_{EO} as an index to tune the hyperparameter and report the results in Appendix D.1. The results illustrate that optimizing hyperparameters using F_{EO} can improve TPR and F_{EO} . This demonstrates the good flexibility and applicability of our methods to different metrics and datasets. We further show the FPR comparison results on FF++ and DFDC datasets

with detailed performance in subgroups in Figure 2. Our methods evidently narrow the disparity between subgroups and lower the FPR of each subgroup.

Performance on Various Detection Models. We further evaluate the effectiveness of our methods on four popular deepfake detection models on the FF++ dataset. The results are presented in Table 5. It is clear that our methods can improve the fairness performance of the detectors without significantly decreasing the detection performance. These results indicate our methods exhibit high scalability and can be seamlessly integrated with different backbones and deepfake detection models.

5. Conclusion

Recent studies have demonstrated the unfairness of deepfake detection. However, solving this issue from an algorithm level has not been extensively studied previously. In this work, we propose two methods, DAG-FDD and DAW-FDD, to train fair deepfake detection models in ways that are agnostic or aware of demographic factors. Extensive experiments on four large-scale deepfake datasets and five deepfake detectors show the effectiveness of our methods in improving the fairness of existing deepfake detectors.

A limitation of our methods is that they rely on the assumption that loss functions can be decomposed into individual terms and that each instance is independent. Therefore, integrating our methods into graph learning-based detectors may not be straightforward.

In future work, we aim to extend this work in the following areas. Firstly, we will examine the fairness generalization abilities of cross-dataset deepfake detection. Secondly, we will investigate fairness methods for managing non-decomposable loss-based detectors.

References

- [1] Deepfakes dataset by google & jigsaw. In <https://ai.googleblog.com/2019/09/contributing-data-to-deepfakedetection.html>, 2019. 2, 5
- [2] Matyáš Boháček and Hany Farid. Protecting world leaders against deep fakes using facial, gestural, and vocal mannerisms. *Proceedings of the National Academy of Sciences*, 119(48):e2216035119, 2022. 1
- [3] Junyi Cao, Chao Ma, Taiping Yao, Shen Chen, Shouhong Ding, and Xiaokang Yang. End-to-end reconstruction-classification learning for face forgery detection. In *Proceedings of the IEEE/CVF Conference on Computer Vision and Pattern Recognition*, pages 4113–4122, 2022. 6
- [4] Simon Caton and Christian Haas. Fairness in machine learning: A survey. *arXiv preprint arXiv:2010.04053*, 2020. 2, 6
- [5] Junyi Chai, Taeuk Jang, and Xiaoqian Wang. Fairness without demographics through knowledge distillation. In *Advances in Neural Information Processing Systems*. 2
- [6] Davide Alessandro Coccomini, Nicola Messina, Claudio Gennaro, and Fabrizio Falchi. Combining efficientnet and vision transformers for video deepfake detection. In *Image Analysis and Processing–ICIAP 2022: 21st International Conference, Lecce, Italy, May 23–27, 2022, Proceedings, Part III*, pages 219–229. Springer, 2022. 1
- [7] Davide Cozzolino, Alessandro Pianese, Matthias Nießner, and Luisa Verdoliva. Audio-visual person-of-interest deepfake detection. In *Proceedings of the IEEE/CVF Conference on Computer Vision and Pattern Recognition*, pages 943–952, 2023. 6
- [8] Prafulla Dhariwal and Alexander Nichol. Diffusion models beat gans on image synthesis. *Advances in Neural Information Processing Systems*, 34:8780–8794, 2021. 1
- [9] Brian Dolhansky, Joanna Bitton, Ben Pfau, Jikuo Lu, Russ Howes, Menglin Wang, and Cristian Canton Ferrer. The deepfake detection challenge (dfdc) dataset. *arXiv preprint arXiv:2006.07397*, 2020. 2, 5
- [10] Shichao Dong, Jin Wang, Renhe Ji, Jiajun Liang, Haoqiang Fan, and Zheng Ge. Implicit identity leakage: The stumbling block to improving deepfake detection generalization. In *Proceedings of the IEEE/CVF Conference on Computer Vision and Pattern Recognition*, pages 3994–4004, 2023. 2
- [11] Xiaoyi Dong, Jianmin Bao, Dongdong Chen, Ting Zhang, Weiming Zhang, Nenghai Yu, Dong Chen, Fang Wen, and Baining Guo. Protecting celebrities from deepfake with identity consistency transformer. In *Proceedings of the IEEE/CVF Conference on Computer Vision and Pattern Recognition*, pages 9468–9478, 2022. 2
- [12] John C Duchi and Hongseok Namkoong. Learning models with uniform performance via distributionally robust optimization. *The Annals of Statistics*, 49(3):1378–1406, 2021. 3, 8
- [13] Cynthia Dwork, Moritz Hardt, Toniann Pitassi, Omer Reingold, and Richard Zemel. Fairness through awareness. In *Proceedings of the 3rd innovations in theoretical computer science conference*, pages 214–226, 2012. 2, 4
- [14] Meiling Fang, Wufei Yang, Arjan Kuijper, Vitomir Struc, and Naser Damer. Fairness in face presentation attack detection. *arXiv preprint arXiv:2209.09035*, 2022. 2
- [15] James R Foulds, Rashidul Islam, Kamrun Naher Keya, and Shimei Pan. An intersectional definition of fairness. In *2020 IEEE 36th International Conference on Data Engineering (ICDE)*, pages 1918–1921. IEEE, 2020. 2
- [16] Ian Goodfellow, Jean Pouget-Abadie, Mehdi Mirza, Bing Xu, David Warde-Farley, Sherjil Ozair, Aaron Courville, and Yoshua Bengio. Generative adversarial networks. *Communications of the ACM*, 63(11):139–144, 2020. 1
- [17] Vincent Grari, Sylvain Lamprier, and Marcin Detyniecki. Fairness without the sensitive attribute via causal variational autoencoder. *IJCAI*, 2022. 2
- [18] Moritz Hardt, Eric Price, and Nati Srebro. Equality of opportunity in supervised learning. *Advances in neural information processing systems*, 29, 2016. 2, 4
- [19] John C Harsanyi. *Rational behaviour and bargaining equilibrium in games and social situations*. Cambridge University Press, 1977. 5
- [20] Tatsunori Hashimoto, Megha Srivastava, Hongseok Namkoong, and Percy Liang. Fairness without demographics in repeated loss minimization. In *International Conference on Machine Learning*, pages 1929–1938. PMLR, 2018. 2, 3, 5, 6, 15
- [21] Caner Hazirbas, Joanna Bitton, Brian Dolhansky, Jacqueline Pan, Albert Gordo, and Cristian Canton Ferrer. Towards measuring fairness in ai: the casual conversations dataset. *IEEE Transactions on Biometrics, Behavior, and Identity Science*, 4(3):324–332, 2021. 1, 2, 3
- [22] Kaiming He, Xiangyu Zhang, Shaoqing Ren, and Jian Sun. Deep residual learning for image recognition. In *Proceedings of the IEEE conference on computer vision and pattern recognition*, pages 770–778, 2016. 6
- [23] Shu Hu, Lipeng Ke, Xin Wang, and Siwei Lyu. Tkml-ap: Adversarial attacks to top-k multi-label learning. In *Proceedings of the IEEE/CVF International Conference on Computer Vision*, pages 7649–7657, 2021. 3
- [24] Felix Juefei-Xu, Run Wang, Yihao Huang, Qing Guo, Lei Ma, and Yang Liu. Countering malicious deepfakes: Survey, battleground, and horizon. *International Journal of Computer Vision*, 130(7):1678–1734, 2022. 1
- [25] Kimmo Karkkainen and Jungseock Joo. Fairface: Face attribute dataset for balanced race, gender, and age for bias measurement and mitigation. In *Proceedings of the IEEE/CVF Winter Conference on Applications of Computer Vision*, pages 1548–1558, 2021. 2
- [26] Kamrun Naher Keya, Rashidul Islam, Shimei Pan, Ian Stockwell, and James Foulds. Equitable allocation of healthcare resources with fair survival models. In *Proceedings of the 2021 siam international conference on data mining (sdm)*, pages 190–198. SIAM, 2021. 7
- [27] Leo Kim. Fake pictures of people of color won’t fix ai bias. In *WIRED*, <https://tinyurl.com/yc4dsyms>, 2023. 1
- [28] Davis E King. Dlib-ml: A machine learning toolkit. *The Journal of Machine Learning Research*, 10:1755–1758, 2009. 5, 15

- [29] Diederik P Kingma and Max Welling. Auto-encoding variational bayes. *arXiv preprint arXiv:1312.6114*, 2013. [1](#)
- [30] Preethi Lahoti, Alex Beutel, Jilin Chen, Kang Lee, Flavien Prost, Nithum Thain, Xuezhi Wang, and Ed Chi. Fairness without demographics through adversarially reweighted learning. *Advances in neural information processing systems*, 33:728–740, 2020. [2](#)
- [31] Daniel Levy, Yair Carmon, John C Duchi, and Aaron Sidford. Large-scale methods for distributionally robust optimization. *Advances in Neural Information Processing Systems*, 33:8847–8860, 2020. [1](#)
- [32] Xiaodan Li, Yining Lang, Yuefeng Chen, Xiaofeng Mao, Yuan He, Shuhui Wang, Hui Xue, and Quan Lu. Sharp multiple instance learning for deepfake video detection. In *Proceedings of the 28th ACM international conference on multimedia*, pages 1864–1872, 2020. [1](#)
- [33] Yuezun Li, Xin Yang, Pu Sun, Honggang Qi, and Siwei Lyu. Celeb-df: A large-scale challenging dataset for deepfake forensics. In *Proceedings of the IEEE/CVF conference on computer vision and pattern recognition*, pages 3207–3216, 2020. [2](#), [5](#), [6](#)
- [34] Siwei Lyu, Yanbo Fan, Yiming Ying, and Bao-Gang Hu. Average top-k aggregate loss for supervised learning. *IEEE Transactions on Pattern Analysis and Machine Intelligence*, 44(1):76–86, 2020. [4](#)
- [35] David Madras, Elliot Creager, Toniann Pitassi, and Richard Zemel. Learning adversarially fair and transferable representations. In *International Conference on Machine Learning*, pages 3384–3393. PMLR, 2018. [2](#)
- [36] Momina Masood, Mariam Nawaz, Khalid Mahmood Malik, Ali Javed, Aun Irtaza, and Hafiz Malik. Deepfakes generation and detection: State-of-the-art, open challenges, countermeasures, and way forward. *Applied Intelligence*, pages 1–53, 2022. [1](#), [3](#)
- [37] Momina Masood, Mariam Nawaz, Khalid Mahmood Malik, Ali Javed, Aun Irtaza, and Hafiz Malik. Deepfakes generation and detection: State-of-the-art, open challenges, countermeasures, and way forward. *Applied Intelligence*, 53(4):3974–4026, 2023. [2](#)
- [38] Ninareh Mehrabi, Fred Morstatter, Nripsuta Saxena, Kristina Lerman, and Aram Galstyan. A survey on bias and fairness in machine learning. *ACM Computing Surveys (CSUR)*, 54(6):1–35, 2021. [1](#), [2](#), [6](#)
- [39] Mehryar Mohri, Gary Sivek, and Ananda Theertha Suresh. Agnostic federated learning. In *International Conference on Machine Learning*, pages 4615–4625. PMLR, 2019. [5](#)
- [40] Aakash Varma Nadimpalli and Ajita Rattani. Gbdf: gender balanced deepfake dataset towards fair deepfake detection. *arXiv preprint arXiv:2207.10246*, 2022. [1](#), [2](#), [3](#), [4](#), [6](#), [15](#)
- [41] Aakash Varma Nadimpalli and Ajita Rattani. On improving cross-dataset generalization of deepfake detectors. In *Proceedings of the IEEE/CVF Conference on Computer Vision and Pattern Recognition*, pages 91–99, 2022. [6](#)
- [42] Huy H Nguyen, Junichi Yamagishi, and Isao Echizen. Use of a capsule network to detect fake images and videos. *arXiv preprint arXiv:1910.12467*, 2019. [1](#)
- [43] Adam Paszke, Sam Gross, Francisco Massa, Adam Lerer, James Bradbury, Gregory Chanan, Trevor Killeen, Zeming Lin, Natalia Gimelshein, Luca Antiga, et al. Pytorch: An imperative style, high-performance deep learning library. *NeurIPS*, 32, 2019. [6](#)
- [44] Muxin Pu, Meng Yi Kuan, Nyee Thoang Lim, Chun Yong Chong, and Mei Kuan Lim. Fairness evaluation in deepfake detection models using metamorphic testing. *arXiv preprint arXiv:2203.06825*, 2022. [2](#), [3](#)
- [45] Hamed Rahimian and Sanjay Mehrotra. Distributionally robust optimization: A review. *arXiv preprint arXiv:1908.05659*, 2019. [1](#)
- [46] Raghavendra Ramachandra, Kiran Raja, and Christoph Busch. Algorithmic fairness in face morphing attack detection. In *Proceedings of the IEEE/CVF Winter Conference on Applications of Computer Vision*, pages 410–418, 2022. [2](#)
- [47] John Rawls. *Justice as fairness: A restatement*. Harvard University Press, 2001. [2](#), [5](#)
- [48] R Tyrrell Rockafellar, Stanislav Uryasev, et al. Optimization of conditional value-at-risk. *Journal of risk*, 2:21–42, 2000. [1](#), [3](#)
- [49] Robin Rombach, Andreas Blattmann, Dominik Lorenz, Patrick Esser, and Björn Ommer. High-resolution image synthesis with latent diffusion models. In *Proceedings of the IEEE/CVF Conference on Computer Vision and Pattern Recognition*, pages 10684–10695, 2022. [1](#)
- [50] Andreas Rossler, Davide Cozzolino, Luisa Verdoliva, Christian Riess, Justus Thies, and Matthias Nießner. Faceforensics++: Learning to detect manipulated facial images. In *Proceedings of the IEEE/CVF international conference on computer vision*, pages 1–11, 2019. [2](#), [5](#), [6](#)
- [51] Shiori Sagawa, Pang Wei Koh, Tatsunori B Hashimoto, and Percy Liang. Distributionally robust neural networks for group shifts: On the importance of regularization for worst-case generalization. *ICLR*, 2020. [6](#), [15](#)
- [52] Mingxing Tan and Quoc Le. Efficientnet: Rethinking model scaling for convolutional neural networks. In *International conference on machine learning*, pages 6105–6114. PMLR, 2019. [6](#)
- [53] Loc Trinh and Yan Liu. An examination of fairness of ai models for deepfake detection. *IJCAI*, 2021. [1](#), [2](#)
- [54] Arash Vahdat and Jan Kautz. Nvae: A deep hierarchical variational autoencoder. *Advances in neural information processing systems*, 33:19667–19679, 2020. [1](#)
- [55] Arash Vahdat, Karsten Kreis, and Jan Kautz. Score-based generative modeling in latent space. *Advances in Neural Information Processing Systems*, 34:11287–11302, 2021. [1](#)
- [56] Jialu Wang, Xin Eric Wang, and Yang Liu. Understanding instance-level impact of fairness constraints. In *International Conference on Machine Learning*, pages 23114–23130. PMLR, 2022. [6](#), [15](#)
- [57] Junke Wang, Zuxuan Wu, Wenhao Ouyang, Xintong Han, Jingjing Chen, Yu-Gang Jiang, and Ser-Nam Li. M2tr: Multi-modal multi-scale transformers for deepfake detection. In *Proceedings of the 2022 International Conference on Multimedia Retrieval*, pages 615–623, 2022. [1](#)

- [58] Tianyi Wang and Kam Pui Chow. Noise based deepfake detection via multi-head relative-interaction. In *Proceedings of the AAAI Conference on Artificial Intelligence*, volume 37, pages 14548–14556, 2023. 6
- [59] Zhendong Wang, Jianmin Bao, Wengang Zhou, Weilun Wang, and Houqiang Li. Altfreezing for more general video face forgery detection. In *Proceedings of the IEEE/CVF Conference on Computer Vision and Pattern Recognition*, pages 4129–4138, 2023. 2
- [60] Kyle Wiggers. Deepfake detectors and datasets exhibit racial and gender bias, usc study shows. In *VentureBeat*, <https://tinyurl.com/ms8zbu6f>, 2021. 1
- [61] Robert Williamson and Aditya Menon. Fairness risk measures. In *International Conference on Machine Learning*, pages 6786–6797. PMLR, 2019. 1, 4, 5, 6, 15
- [62] Ying Xu, Philipp Terhörst, Kiran Raja, and Marius Pederesen. A comprehensive analysis of ai biases in deepfake detection with massively annotated databases. *arXiv preprint arXiv:2208.05845*, 2022. 1, 2, 3, 4, 5
- [63] Shen Yan, Hsien-te Kao, and Emilio Ferrara. Fair class balancing: Enhancing model fairness without observing sensitive attributes. In *Proceedings of the 29th ACM International Conference on Information & Knowledge Management*, pages 1715–1724, 2020. 2
- [64] Jun Yu, Xinlong Hao, Haonian Xie, and Ye Yu. Fair face recognition using data balancing, enhancement and fusion. In *European Conference on Computer Vision*, pages 492–505. Springer, 2020. 2
- [65] Runtian Zhai, Chen Dan, Zico Kolter, and Pradeep Ravikumar. Doro: Distributional and outlier robust optimization. In *International Conference on Machine Learning*, pages 12345–12355. PMLR, 2021. 3, 7
- [66] Hanqing Zhao, Wenbo Zhou, Dongdong Chen, Tianyi Wei, Weiming Zhang, and Nenghai Yu. Multi-attentional deepfake detection. In *Proceedings of the IEEE/CVF conference on computer vision and pattern recognition*, pages 2185–2194, 2021. 1, 2
- [67] Tianxiang Zhao, Enyan Dai, Kai Shu, and Suhang Wang. Towards fair classifiers without sensitive attributes: Exploring biases in related features. In *Proceedings of the Fifteenth ACM International Conference on Web Search and Data Mining*, pages 1433–1442, 2022. 2

Appendix for “Improving Fairness in Deepfake Detection”

This Appendix provides proof of the proposed methods, additional experimental details and results. Specifically, Sections A and B provide proof and details of the proposed methods. Section C provides details of our experiment, including parameter setting and source code. Section D provides further analysis of additional experimental results, including optimization by different metric (in D.1), effect of choosing different hyperparameters (in D.2), performance on Cross-domain Dataset (in D.3), convergence analysis of the proposed methods (in D.4), more comparison results (in D.5 and D.6), and details on datasets and results of each subgroup (in D.7 and D.8).

A. Proofs

A.1. Proof of Proposition 1

Proof. For any m , denote $Z = (X, Y)$ and \mathcal{D}_m as a set that contains samples from m -th group, then $\mathbb{P}(Z) = \pi_m \mathbb{P}(Z|\mathcal{D}_m) + (1 - \pi_m) \mathbb{P}(Z|\overline{\mathcal{D}_m})$, where $\overline{\mathcal{D}_m}$ contains samples are not in \mathcal{D}_m . Let $\mathbb{Q}(Z) = \mathbb{P}(Z|\mathcal{D}_m)$ and $\mathbb{Q}'(Z) = \frac{\pi_m - \alpha}{1 - \alpha} \mathbb{P}(Z|\mathcal{D}_m) + \frac{1 - \pi_m}{1 - \alpha} \mathbb{P}(Z|\overline{\mathcal{D}_m})$. Then $\mathbb{P}(Z) = \alpha \mathbb{Q}(Z) + (1 - \alpha) \mathbb{Q}'(Z)$, which implies that

$$\alpha \mathbb{E}_{\mathbb{Q}(Z)}[\ell(\theta; Z) - \lambda] = \mathbb{E}_{\alpha \mathbb{Q}(Z)}[\ell(\theta; Z) - \lambda] \leq \mathbb{E}_{\alpha \mathbb{Q}(Z)}[[\ell(\theta; Z) - \lambda]_+] \leq \mathbb{E}_{\mathbb{P}(Z)}[[\ell(\theta; Z) - \lambda]_+].$$

The last inequality holds because $\alpha \leq \min_{m=1, \dots, K} \pi_m$ and $\alpha \in (0, 1)$, which means $\mathbb{Q}'(Z) \geq 0$ and therefore $\mathbb{P}(Z) \geq \alpha \mathbb{Q}(Z)$. From the above inequations, we obtain

$$\begin{aligned} \alpha \mathbb{E}_{\mathbb{Q}(Z)}[\ell(\theta; Z) - \lambda] &\leq \mathbb{E}_{\mathbb{P}(Z)}[[\ell(\theta; Z) - \lambda]_+] \\ \Rightarrow \mathbb{E}_{\mathbb{Q}(Z)}[\ell(\theta; Z) - \lambda] &\leq \frac{1}{\alpha} \mathbb{E}_{\mathbb{P}(Z)}[[\ell(\theta; Z) - \lambda]_+] \\ \Rightarrow \mathbb{E}_{\mathbb{Q}(Z)}[\ell(\theta; Z)] &\leq \lambda + \frac{1}{\alpha} \mathbb{E}_{\mathbb{P}(Z)}[[\ell(\theta; Z) - \lambda]_+] = \text{CVaR}_\alpha(\theta) \end{aligned}$$

In Section 3.1, we have already defined \mathbb{P}_m , which is just $\mathbb{Q}(Z)$. Therefore, we have $\mathcal{R}_{\max}(\theta) \leq \text{CVaR}_\alpha(\theta)$. □

A.2. Proof of Theorem 1

Proof. 1) We first prove that $\frac{1}{k} \sum_{i=1}^k \ell_{[i]} = \min_{\lambda \in \mathbb{R}} \lambda + \frac{1}{k} \sum_{i=1}^n [\ell_i - \lambda]_+$.
 \Rightarrow : Suppose $\bar{\ell} := \{\ell_1, \dots, \ell_n\}$. We know $\sum_{i=1}^k \ell_{[i]}$ is the solution of

$$\max_{\mathbf{p}} \mathbf{p}^\top \bar{\ell}, \text{ s.t. } \mathbf{p}^\top \mathbf{1} = k, \mathbf{0} \leq \mathbf{p} \leq \mathbf{1}.$$

We apply Lagrangian to this equation and get

$$\mathcal{L} = -\mathbf{p}^\top \bar{\ell} - \mathbf{v}^\top \mathbf{p} + \mathbf{u}^\top (\mathbf{p} - \mathbf{1}) + \lambda (\mathbf{p}^\top \mathbf{1} - k)$$

where $\mathbf{u} \geq \mathbf{0}$, $\mathbf{v} \geq \mathbf{0}$ and $\lambda \in \mathbb{R}$ are Lagrangian multipliers. Taking its derivative with respect to \mathbf{p} and set it to 0, we have $\mathbf{v} = \mathbf{u} - \bar{\ell} + \lambda \mathbf{1}$. Substituting it back into the Lagrangian, we get

$$\min_{\mathbf{u}, \lambda} \mathbf{u}^\top \mathbf{1} + k\lambda, \text{ s.t. } \mathbf{u} \geq \mathbf{0}, \mathbf{u} + \lambda \mathbf{1} - \bar{\ell} \geq \mathbf{0}.$$

This means

$$\sum_{i=1}^k \ell_{[i]} = \min_{\lambda} k\lambda + \sum_{i=1}^n [\ell_i - \lambda]_+.$$

Therefore,

$$\frac{1}{k} \sum_{i=1}^k \ell_{[i]} = \min_{\lambda} \lambda + \frac{1}{k} \sum_{i=1}^n [\ell_i - \lambda]_+. \tag{A.1}$$

\Leftarrow : Denote $\bar{\mathcal{L}} := \lambda + \frac{1}{k} \sum_{i=1}^n [\ell_i - \lambda]_+$. Since $\bar{\mathcal{L}}$ is a convex function with respect to λ , we can set the $\partial_\lambda \bar{\mathcal{L}} = 0$ to get the optimal value of λ^* . Thus, we have $\partial_\lambda \bar{\mathcal{L}} = 1 - \frac{1}{k} \sum_{i=1}^n \mathbb{I}_{[\ell_i \geq \lambda^*]} = 0$, then $\lambda^* = \ell_{[k]}$ can be an optimal value. Taking $\lambda^* = \ell_{[k]}$ into $\bar{\mathcal{L}}$, we obtain $\bar{\mathcal{L}} = \frac{1}{k} \sum_{i=1}^k \ell_{[i]}$.

Based on the above analysis, we get $\frac{1}{k} \sum_{i=1}^k \ell_{[i]} = \min_{\lambda \in \mathbb{R}} \lambda + \frac{1}{k} \sum_{i=1}^n [\ell_i - \lambda]_+$.

2) Using the above result, we can directly replace $L_i(\theta) = \frac{1}{k_i} \sum_{j=1}^{k_i} \ell_{[j]}^{g_i}(\theta)$ from (5) with $L_i(\theta) = \min_{\lambda_i \in \mathbb{R}} \lambda_i + \frac{1}{\alpha_i |g_i|} \sum_{j:S_j=g_i} [\ell(\theta; X_j, Y_j) - \lambda_i]_+$, where $k_i = \alpha_i |g_i|$. This has also shown in (6). \square

B. Explicit Forms of (sub)gradients

From equation (6), we have

$$\begin{aligned} \min_{\theta, \lambda \in \mathbb{R}} \mathcal{L}_{\text{DAW-FDD}}(\theta, \lambda) &:= \lambda + \frac{1}{\alpha |\mathcal{G}|} \sum_{i=1}^{|\mathcal{G}|} [L_i(\theta) - \lambda]_+, \\ \text{s.t. } L_i(\theta) &= \min_{\lambda_i \in \mathbb{R}} L_i(\theta, \lambda_i) := \lambda_i + \frac{1}{\alpha_i |g_i|} \sum_{j:S_j=g_i} [\ell(\theta; X_j, Y_j) - \lambda_i]_+. \end{aligned}$$

We can get

$$\partial_\theta \mathcal{L}_{\text{DAW-FDD}}(\theta, \lambda) = \frac{1}{\alpha |\mathcal{G}|} \sum_{i=1}^{|\mathcal{G}|} \left[\left(\frac{1}{\alpha_i |g_i|} \sum_{j:S_j=g_i} \partial_\theta \ell(\theta; X_j, Y_j) \cdot \mathbb{I}_{[\ell(\theta; X_j, Y_j) > \lambda_i]} \right) \cdot \mathbb{I}_{[L_i(\theta) > \lambda]} \right]$$

C. Additional Experimental Details

C.1. Source Code

For the purpose of review, the source code is accessible in the supplementary file, named as ‘‘Code71’’.

C.2. α and α_i Settings on Each Dataset

We tune α and α_i on the following hyperparameter grid: 0.1, 0.3, 0.5, 0.7, 0.9. We provide a reference for setting α and α_i to reproduce our experimental results in Table C.1.

Parameter	Xception				ResNet-50	EfficientNet-B3	DSP-FWA	RECCE
	FF++	Celeb-DF	DFD	DFDC	FF++	FF++	FF++	FF++
α in DAG-FDD	0.5	0.5	0.3	0.7	0.5	0.5	0.5	0.5
α, α_i in DAW-FDD	0.5, 0.9	0.5, 0.7	0.7, 0.9	0.5, 0.7	0.5, 0.9	0.5, 0.9	0.7, 0.9	0.5, 0.9

Table C.1. Hyperparameter settings of DAG-FDD and DAW-FDD.

C.3. Trade-off Parameters for *Cons.* EFPR and *Cons.* EO

For *Cons.* EFPR and *Cons.* EO baselines, we tune the trade-off hyperparameters on the following grid: 0.5, 0.6, 0.7, 0.8, 0.9. Finally, we use 0.6 for both methods since this hyperparameter can return the best performance.

D. Additional Experimental Results

D.1. Optimization by Metric F_{EO}

We employ F_{EO} as an index to tune the hyperparameter and report the results in Table D.1. The results illustrate that optimizing hyperparameters using F_{EO} can improve TPR and F_{EO} (compared with results in Table 4), which demonstrates that our method can generalize to different metric.

Methods	Fairness Metrics (%) ↓				Detection Metrics (%)			
	Intersection				Overall			
	G_{AUC}	G_{FPR}	F_{FPR}	F_{EO}	AUC ↑	FPR ↓	TPR ↑	ACC ↑
Original	8.53	11.81	15.66	39.95	97.17	13.01	95.83	94.05
DAG-FDD (Ours)	5.86	7.04	8.23	29.65	98.50	5.06	93.48	93.78
DAW-FDD (Ours)	6.67	2.96	3.96	30.52	98.81	2.78	91.99	93.04

Table D.1. Test set results of Xception on the Celeb-DF dataset, optimized by F_{EO} metric.

D.2. Effect of α and α_i

Fig. D.1 shows the fairness metrics and performance metric AUC to different α and α_i values in DAG-FDD and DAW-FDD methods, respectively, when using Xception as backbone in FF++ dataset. Experiment result in Fig. D.1 (a) demonstrates that the model achieves the best fairness performance when setting α as 0.5 in DAG-FDD and also keeps fair AUC score. In FAW-FDD, we set α as 0.5 selected from the range of $\{0.1, 0.3, 0.5, 0.7, 0.9\}$ based on the best fairness performance first. Secondly, we searched for the optimal value of α_i in the range of $\{0.1, 0.3, 0.5, 0.7, 0.9\}$ while keeping α fixed at its optimal value. Fig. D.1 (b) shows that the proposed DAW-FDD performs best when α_i is set to 0.9 when α is fixed on 0.5.

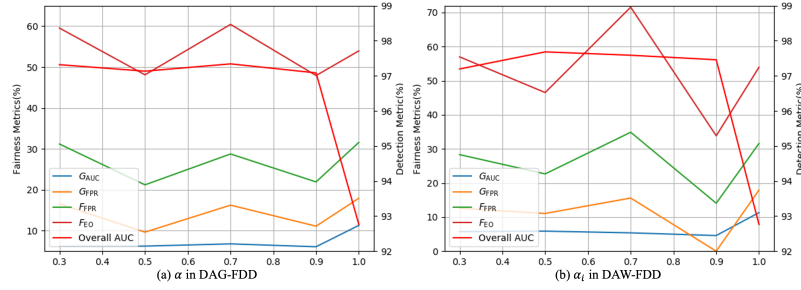


Figure D.1. Parameters of DAG-FDD and DAW-FDD on FF++ dataset with Xception.

D.3. Performance on Cross-domain Dataset

We further evaluate the performance of our methods using Xception on cross-domain dataset. The models are trained on FF++ dataset and tested on DFDC dataset. The results are presented in Table D.2.

Methods	Fairness Metrics (%) ↓				Detection Metrics (%)			
	Intersection				Overall			
	G_{AUC}	G_{FPR}	F_{FPR}	F_{EO}	AUC ↑	FPR ↓	TPR ↑	ACC ↑
Original	33.76	17.19	30.70	122.51	58.81	59.54	71.60	51.57
DAG-FDD (Ours)	25.42	24.16	49.27	117.19	56.32	35.29	47.06	58.41
DAW-FDD (Ours)	26.96	21.50	45.34	119.32	59.95	43.70	60.69	57.87

Table D.2. Cross-domain Performance. Models are trained on FF++ and tested on DFDC.

D.4. Convergence of the Proposed Loss Functions

We also show the training loss convergence of our methods when applying to Xception on FF++ dataset in Fig. D.2. The results show that our methods can converge within reasonable epochs.

D.5. Comparison on SOTA Deepfake Detector

Since the RECCE model achieves SOTA detection performance on several datasets, we apply our methods and baselines based on the RECCE detector and show the results in Table D.3. The results demonstrate the adaptability and efficiency of our methods.

D.6. Results on DF-Platter Dataset

We apply our methods and baseline to the Xception network on a recent Deepfake dataset with demographic annotations, namely DF-Platter, to further illustrate the effectiveness of our methods. We mainly consider Gender (Male and Female) and

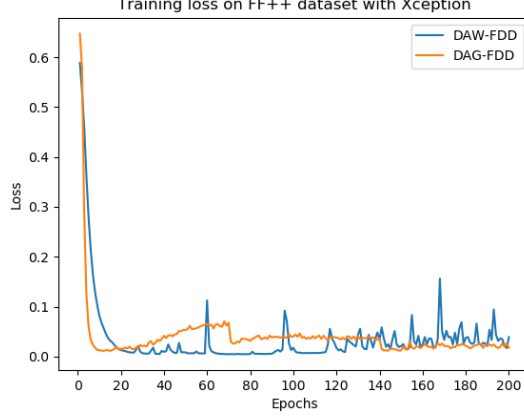


Figure D.2. Training loss convergence.

Methods	Require Demo-graphics	Fairness Metrics (%) ↓									Detection Metrics (%)			
		Gender			Race			Intersection			Overall			
		G_{FPR}	F_{FPR}	F_{EO}	G_{FPR}	F_{FPR}	F_{EO}	G_{FPR}	F_{FPR}	F_{EO}	AUC ↑	FPR ↓	TPR ↑	ACC ↑
Original	—	0.87	0.87	3.14	18.81	27.65	30.07	30.26	67.38	80.34	98.05	21.20	98.21	94.74
DRO χ^2 [20]	×	1.46	1.46	4.17	13.87	20.05	23.15	23.63	42.14	57.29	98.32	15.65	97.28	94.97
DAG-FDD (Ours)		0.55	0.55	3.71	12.68	17.41	20.33	15.40	36.17	54.24	98.33	12.01	96.80	95.23
Naive [40]	✓	9.48	9.48	13.05	18.26	20.86	22.27	28.74	73.59	89.87	93.64	27.57	95.96	91.76
FRM [61]		2.15	2.15	5.48	8.50	10.00	13.75	14.88	30.59	49.86	98.06	15.21	97.05	94.86
Group DRO [51]		0.74	0.74	3.71	12.08	16.26	20.01	15.17	32.95	51.08	98.22	11.75	96.59	95.10
Cons. EFPR [56]		6.13	6.13	11.15	10.71	15.00	19.46	13.67	38.48	63.80	97.17	14.72	96.29	94.32
DAW-FDD (Ours)		0.25	0.25	4.75	6.99	7.96	11.95	13.54	23.44	52.95	98.35	8.15	94.59	94.10

Table D.3. Comparison results with different fairness solutions using RECCE Deepfake detector on FF++ testing set across Gender, Race, and Intersection groups. The best results are shown in **Bold**. ↑ means higher is better and ↓ means lower is better. Gray highlights mean our methods outperform the baselines in the group (i.e., DAG-FDD vs. Original/DRO χ^2 , DAW-FDD vs. Original/Naive/FRM/Group DRO/Cons. EFPR).

Methods	Fairness Metrics (%) ↓									Detection Metrics (%)			
	Gender			Age			Intersection			Overall			
	G_{FPR}	F_{FPR}	F_{EO}	G_{FPR}	F_{FPR}	F_{EO}	G_{FPR}	F_{FPR}	F_{EO}	AUC ↑	FPR ↓	TPR ↑	ACC ↑
Original	3.70	3.70	3.92	3.43	3.90	5.03	4.96	11.94	14.56	99.93	2.80	99.82	98.54
DAG-FDD (Ours)	3.05	3.05	3.18	3.40	3.29	4.06	4.72	10.35	12.03	99.97	2.42	99.91	98.77
DAW-FDD (Ours)	1.95	1.95	2.13	1.97	2.17	2.96	3.27	6.81	8.81	99.97	1.75	99.82	99.05

Table D.4. Comparison results with different fairness solutions using the Xception detector on DF-Platter testing set across Gender, Age, and Intersection groups. The best results are shown in **Bold**. ↑ means higher is better and ↓ means lower is better. Gray highlights mean our methods outperform the Original baseline.

Age (Young Adult, Adult, Old) attributes based on the official annotations. In addition to the single attribute fairness, we also consider the combined attributes (Intersection) group, including Male-Young Adult (M-Y), Male-Adult (M-A), Male-Old (M-O), Female-Young Adult (F-Y), Female-Adult (F-A), and Female-Old (F-O). We train and evaluate our methods on a subset of the DF-Platter dataset consisting of real and FSGAN-generated data from Set A with C23 compression, and use Dlib [28] for face extraction and alignment. The cropped faces are resized to 380×380 for training and testing. Training/validation/test datasets are divided following the official split, without identity overlapping. Experiment results shown in Table D.4 demonstrate that our methods outperform baseline for most metrics.

D.7. Dataset Details

We show the total number of train/val/test samples of each dataset and the attributes included in our experiment in Table D.5. Specifically, the number of training samples within each subgroup for four datasets is shown in Table D.6.

Dataset	# Samples	Sensitive Attributes
FF++	126,956	Gender (Male, Female), Race (White, Black, Asian, Others)
Celeb-DF	143,273	Gender (Male, Female), Race (White, Black, Others)
DFD	40,246	Gender (Male, Female), Race (White, Black, Others)
DFDC	117,065	Gender (Male, Female), Race (White, Black, Asian, Others)

Table D.5. *Sample number and attributes in each dataset.*

Datasets	Gender		Race				Intersection							
	M	F	A	B	W	O	M-A	M-B	M-W	M-O	F-A	F-B	F-W	F-O
FF++	33549	42590	10488	2579	56724	6348	2475	1468	31281	4163	8013	1111	31281	2185
Celeb-DF	87344	6251	-	630	86583	6382	-	600	81194	5550	-	30	5389	832
DFD	16607	7227	-	8121	11911	3802	-	6482	7784	2341	-	1639	4127	1461
DFDC	37911	33567	4059	18909	40257	8253	2144	9603	21755	4409	1915	9306	18502	3844

Table D.6. *Number of training samples of each group in the FF++, Celeb-DF, DFD and DFDC datasets. “-” means group does not exist in the dataset.*

D.8. Detailed Results

Detailed test results of each subgroup on four datasets based on four models are presented in this section. Table D.7 provides comprehensive metrics of each subgroup on the four datasets, while Table D.8 displays details of the four models. These findings align with the results reported in Tables 2, 4, 5 and Figures 1, 2 of the submitted manuscript.

Datasets	Methods	Metric (%)	Gender		Race				Intersection							
			M	F	A	B	W	O	M-A	M-B	M-W	M-O	F-A	F-B	F-W	F-O
FF++	Original	AUC	92.42	93.30	89.33	94.44	92.93	97.01	88.09	95.21	92.47	95.43	90.33	93.42	93.53	99.40
		FPR	19.86	23.95	32.67	24.29	20.10	19.58	25.63	21.74	19.01	18.79	36.72	26.27	21.08	20.53
		TPR	91.84	96.80	94.92	95.66	94.09	96.07	89.13	95.69	91.70	93.43	97.96	95.63	96.35	99.86
		ACC	89.80	93.01	89.55	92.17	91.57	93.49	86.12	93.02	89.83	91.55	91.38	91.30	93.20	96.20
	DAG-FDD (Ours)	AUC	96.59	97.65	96.74	96.76	97.08	98.76	93.20	99.44	96.55	98.34	98.24	94.19	97.60	99.31
		FPR	8.67	10.30	13.65	8.57	9.21	5.42	14.29	9.78	8.06	6.08	13.29	7.63	10.26	4.64
		TPR	91.93	96.51	94.62	95.25	94.28	93.63	88.16	98.43	92.06	91.11	98.02	91.88	96.39	97.25
		ACC	91.82	95.26	93.01	94.58	93.66	93.79	87.66	97.18	92.04	91.55	95.86	91.97	95.19	96.91
	DAW-FDD (Ours)	AUC	96.91	98.05	96.39	97.92	97.54	98.23	94.63	97.81	97.07	97.24	97.35	98.23	98.11	99.22
		FPR	11.29	11.61	12.58	13.33	11.18	10.84	9.24	15.22	11.20	12.71	14.49	11.86	11.17	8.61
		TPR	93.48	97.15	94.40	96.36	95.47	95.77	88.91	96.08	93.92	93.13	97.29	96.67	96.94	99.57
		ACC	92.65	95.55	93.04	94.67	94.29	94.68	89.29	94.35	93.02	92.23	95.05	94.98	95.48	98.10
Celeb-DF	Original	AUC	87.83	98.04	-	91.47	97.40	99.91	-	91.47	-	-	-	-	98.00	100
		FPR	16.47	11.55	-	11.55	13.31	10.00	-	11.55	-	-	-	-	11.81	0.00
		TPR	79.62	96.74	-	79.62	96.74	100	-	79.62	-	-	-	-	96.74	100
		ACC	81.90	95.44	-	82.88	94.89	91.67	-	82.88	-	-	-	-	95.42	100
	DAG-FDD (Ours)	AUC	91.61	98.53	-	92.56	98.28	99.98	-	92.56	-	-	-	-	98.51	100
		FPR	3.84	1.82	-	2.54	2.43	1.33	-	2.54	-	-	-	-	1.86	0.00
		TPR	73.43	88.18	-	73.43	88.16	100	-	73.43	-	-	-	-	88.16	100
		ACC	86.68	89.75	-	82.31	89.90	98.89	-	82.31	-	-	-	-	89.71	100
	DAW-FDD (Ours)	AUC	88.72	98.93	-	91.52	98.38	100	-	91.52	-	-	-	-	98.91	100
		FPR	4.78	0.97	-	3.80	1.90	0.33	-	3.80	-	-	-	-	0.99	0.00
		TPR	70.22	85.33	-	70.22	85.31	100	-	70.22	-	-	-	-	85.31	100
		ACC	84.79	87.49	-	79.81	87.67	99.44	-	79.81	-	-	-	-	87.43	100
DFD	Original	AUC	92.41	93.34	-	95.27	92.12	-	-	94.12	90.85	-	-	98.39	93.10	-
		FPR	23.44	26.39	-	19.48	26.83	-	-	19.65	26.78	-	-	18.18	26.86	-
		TPR	94.57	97.14	-	96.32	95.95	-	-	94.33	94.41	-	-	100	97.25	-
		ACC	88.36	89.68	-	88.37	88.48	-	-	86.22	88.86	-	-	95.48	88.20	-
	DAG-FDD (Ours)	AUC	92.68	93.93	-	94.93	92.89	-	-	93.64	92.26	-	-	98.51	93.58	-
		FPR	26.53	29.44	-	23.51	29.59	-	-	23.75	28.98	-	-	21.59	29.89	-
		TPR	95.26	97.14	-	97.11	96.13	-	-	95.75	94.96	-	-	99.62	97.13	-
		ACC	87.75	88.72	-	86.73	87.70	-	-	84.44	88.69	-	-	94.35	86.99	-
	DAW-FDD (Ours)	AUC	92.38	93.77	-	94.55	92.68	-	-	93.23	91.93	-	-	98.47	93.42	-
		FPR	27.01	28.41	-	25.97	28.34	-	-	26.54	27.43	-	-	21.59	28.79	-
		TPR	94.97	96.71	-	96.84	95.86	-	-	95.55	94.64	-	-	99.25	96.90	-
		ACC	87.39	88.75	-	85.36	87.93	-	-	82.74	88.86	-	-	94.07	87.26	-
DFDC	Original	AUC	91.19	93.41	79.27	94.69	92.24	89.33	66.96	92.61	92.67	86.82	99.77	95.50	91.54	94.58
		FPR	8.04	6.40	9.30	5.28	7.72	8.67	20.96	4.98	6.61	13.02	0.80	5.57	9.09	0.99
		TPR	74.69	77.41	56.68	81.36	76.45	68.15	44.44	71.80	77.80	67.57	93.33	85.14	75.45	68.61
		ACC	86.90	86.83	87.31	90.66	85.72	84.00	73.36	90.34	87.91	82.22	98.94	90.90	83.53	86.44
	DAG-FDD (Ours)	AUC	90.70	94.22	82.44	95.79	92.00	89.73	69.71	94.49	91.18	87.02	99.63	96.29	92.22	95.60
		FPR	7.22	5.91	6.81	3.87	7.60	8.47	15.28	3.49	6.54	12.54	0.64	4.24	8.91	1.28
		TPR	71.97	76.04	52.50	80.92	74.74	62.38	42.22	70.41	74.85	64.36	83.33	85.06	74.67	60.77
		ACC	86.69	86.54	89.14	91.51	85.09	82.32	77.74	91.25	86.92	81.80	98.63	91.70	83.25	83.03
	DAW-FDD (Ours)	AUC	93.30	96.24	88.66	98.23	93.64	93.69	77.89	96.73	93.24	91.43	100	98.97	93.87	97.72
		FPR	5.06	3.34	4.88	1.95	5.43	4.31	11.35	3.04	4.99	6.27	0.16	0.91	5.97	0.85
		TPR	74.11	75.77	54.17	82.59	74.74	65.15	40.00	74.56	76.92	65.35	96.67	85.76	73.14	64.99
		ACC	88.84	87.93	91.05	93.36	86.36	86.04	80.66	92.45	88.65	86.77	99.70	94.03	84.06	85.03

Table D.7. Detailed test set results of each group in Xception on the FF++, Celeb-DF, DFD and DFDC datasets. '-' means not applicable.

Models	Methods	Metric (%)	Gender		Race				Intersection							
			M	F	A	B	W	O	M-A	M-B	M-W	M-O	F-A	F-B	F-W	F-O
ResNet-50	Original	AUC	93.54	95.15	92.19	96.38	94.51	96.10	87.06	97.67	94.22	94.04	94.75	96.16	94.92	98.23
		FPR	24.57	27.15	33.28	27.62	24.97	20.48	35.29	20.65	23.16	24.86	32.13	33.05	26.61	15.23
		TPR	94.24	98.30	96.89	97.68	96.17	96.49	93.65	96.67	94.17	94.04	98.59	98.75	98.06	100
		ACC	90.96	93.65	91.01	93.25	92.42	93.69	87.75	94.02	91.15	91.12	92.76	92.48	93.60	97.27
	DAG-FDD (Ours)	AUC	93.50	95.56	92.40	95.21	94.69	96.58	89.36	97.17	93.78	94.82	93.92	94.82	95.70	98.82
		FPR	21.33	23.54	27.76	26.67	21.32	21.69	27.31	17.39	20.20	25.41	28.02	33.90	22.34	17.22
		TPR	93.16	97.32	96.48	95.96	95.03	96.01	93.86	95.88	92.83	93.64	97.85	96.04	97.10	99.42
		ACC	90.64	93.51	91.76	92.00	92.12	93.09	89.55	93.85	90.56	90.69	92.94	90.13	93.59	96.43
	DAW-FDD (Ours)	AUC	92.78	94.78	91.78	95.79	93.84	95.50	88.59	96.75	93.17	93.23	93.29	95.93	94.80	97.81
		FPR	21.52	25.31	29.29	23.81	22.55	22.29	29.83	19.57	19.76	27.07	28.99	27.12	25.07	16.56
		TPR	90.29	96.72	94.66	95.66	93.20	95.00	90.74	94.90	89.75	91.62	96.72	96.46	96.46	99.86
		ACC	88.23	92.69	90.00	92.25	90.40	92.15	86.55	92.69	88.09	88.73	91.84	91.81	92.57	96.91
EfficientNet-B3	Original	AUC	94.72	97.07	94.56	98.80	95.96	96.85	90.78	98.64	94.87	96.37	96.59	99.00	97.03	98.29
		FPR	19.19	21.17	25.61	19.05	19.65	16.57	24.79	18.48	19.13	12.71	26.09	19.49	20.11	21.19
		TPR	96.07	98.25	97.33	99.19	97.19	96.07	93.00	99.02	96.56	93.74	99.60	99.38	97.78	99.42
		ACC	93.42	94.70	92.86	96.00	94.20	93.99	89.37	96.35	93.83	92.74	94.73	95.65	94.55	95.72
	DAG-FDD (Ours)	AUC	97.01	97.46	96.06	99.45	97.27	97.73	94.67	99.74	97.08	97.26	96.68	99.19	97.51	98.81
		FPR	8.14	8.61	10.43	0.95	8.46	8.43	9.66	0.00	8.37	8.29	10.87	1.70	8.55	8.61
		TPR	90.32	95.20	93.77	94.34	92.50	94.05	86.55	94.71	90.48	90.40	97.57	93.96	94.40	99.28
		ACC	90.59	94.51	92.95	95.17	92.33	93.64	87.32	95.52	90.68	90.61	95.97	94.82	93.87	97.86
	DAW-FDD (Ours)	AUC	95.96	96.68	95.80	98.09	96.22	97.79	95.09	97.45	95.83	97.20	95.92	98.69	96.68	98.88
		FPR	8.24	8.20	9.51	9.05	8.16	5.72	8.82	11.96	8.24	5.53	9.90	6.78	8.09	5.96
		TPR	88.55	94.05	93.36	95.15	90.68	92.98	86.44	93.73	88.34	89.50	97.00	96.67	92.90	97.97
		ACC	89.11	93.64	92.80	94.42	90.89	93.19	87.40	92.86	88.93	90.27	95.69	95.99	92.72	97.27
DSP-FWA	Original	AUC	89.75	93.97	90.13	95.60	91.72	94.16	83.99	96.38	90.10	90.63	93.32	96.51	93.62	98.77
		FPR	28.48	34.37	40.64	31.43	29.58	34.94	38.24	20.65	26.50	37.02	42.03	39.83	32.37	32.45
		TPR	90.08	95.99	95.33	96.77	92.46	94.11	91.82	95.29	89.48	90.30	97.17	98.33	95.28	99.57
		ACC	86.85	90.45	88.33	91.83	88.55	89.31	85.69	92.86	86.70	86.08	89.73	90.80	90.29	93.82
	DAG-FDD (Ours)	AUC	90.19	92.78	89.50	95.43	91.79	91.83	84.10	95.13	90.78	91.04	92.08	96.06	92.90	93.54
		FPR	29.86	34.50	42.64	37.14	30.11	31.63	42.86	41.30	27.25	29.83	42.51	33.90	32.71	33.78
		TPR	91.02	96.15	94.96	98.59	93.14	93.99	88.38	98.63	90.98	89.90	98.42	98.54	95.18	99.86
		ACC	87.39	90.55	87.64	92.33	89.01	89.76	82.01	92.53	87.80	86.85	90.65	92.14	90.15	93.82
	DAW-FDD (Ours)	AUC	88.15	93.54	90.54	94.44	90.63	92.05	85.08	95.23	87.81	91.13	94.30	93.86	93.49	94.07
		FPR	28.81	31.83	34.20	31.43	29.19	34.94	26.05	38.04	27.88	35.91	38.89	26.27	30.37	33.78
		TPR	87.64	95.92	92.73	96.06	91.22	95.18	82.35	95.88	87.10	92.42	98.19	96.25	95.12	99.13
		ACC	84.77	90.85	87.49	91.25	87.60	90.21	80.63	90.70	84.49	88.04	91.16	91.81	90.52	93.22
RECCE	Original	AUC	97.15	98.86	97.44	98.65	98.12	98.51	94.75	99.20	97.31	97.76	98.71	98.40	98.89	99.71
		FPR	21.67	20.80	32.67	28.10	19.26	13.86	39.50	41.30	19.07	11.05	28.74	17.80	19.43	17.22
		TPR	97.03	99.29	98.04	100	98.17	97.80	95.37	100	97.10	96.47	99.43	100	99.18	99.71
		ACC	93.77	95.62	92.06	95.08	95.08	95.88	88.26	93.69	94.29	95.30	94.09	96.49	95.82	96.67
	DAG-FDD (Ours)	AUC	97.71	98.90	97.13	99.65	98.40	99.04	94.02	99.69	97.97	98.09	98.56	99.62	98.85	99.88
		FPR	11.71	12.26	18.87	6.19	11.45	7.83	19.75	4.35	11.08	10.50	18.36	7.63	11.80	4.64
		TPR	95.15	98.31	96.55	98.79	96.79	96.13	92.47	99.22	95.35	94.04	98.70	98.33	98.16	99.13
		ACC	93.95	96.38	93.55	97.92	95.33	95.48	89.97	98.67	94.23	93.34	95.46	97.16	96.36	98.45
	DAW-FDD (Ours)	AUC	97.73	98.98	98.17	98.85	98.27	99.00	95.52	98.24	97.94	98.31	99.54	99.49	98.70	99.89
		FPR	8.29	8.04	7.67	10.00	8.64	3.01	7.56	16.30	8.56	2.76	7.73	5.09	8.72	3.31
		TPR	92.24	96.74	93.70	97.37	94.60	94.29	85.79	98.24	92.81	90.81	97.85	96.46	96.29	99.28
		ACC	92.15	95.86	93.43	96.08	94.02	94.73	87.15	96.01	92.57	91.80	96.79	96.15	95.38	98.81

Table D.8. Detailed test set results of each group in ResNet-50, EfficientNet-B3, DSP-FWA, and RECCE on the FF++ dataset.